CONF-8410209--1

DE85 006991

Structural Code Benchmarking for the Analysis of Impact Response of Nuclear Material Shipping Casks *

R. E. Glass

ABSTRACT

The Transportation Technology Center at Sandia National Laboratories has initiated a program to benchmark thermal and structural codes that are available to the nuclear material transportation community. The program consists of the following five phrases: 1) code inventory and review, 2) development of a cask-like set of problems, 3) multiple independent numerical analyses of the problems, 4) transfer of information, and 5) performance of experiments to obtain data for comparison with the numerical analyses. This paper will summarize the results obtained by the independent numerical analyses.

The analyses indicate the variability that can be expected both due to differences in user-controlled parameters and from code-to-code differences. The results show that in purely elastic analyses, differences can be attributed to user controlled parameters. Model problems involving elastic/plastic material behavior and large deformations, however, have greater variability with significant differences reported for implicit and explicit integration schemes in finite element programs. This variability demonstrates the need to obtain experimental data to properly benchmark codes utilizing elastic/plastic material models and large deformation capability.

Acknowledgements: The author would like to express his appreciation to the individual contributions that are incorporated in this summary report. These are: John Friley, Battelle, Pacific Northwest Laboratories; Kenneth Gwinn, Sandia National Laboratories; Brett Lewis, Aptek; P. Rasmusson and R. Grenier, GA Technologies; and Hideo Obata and Masaharu Itoh, Century Research Center Corporation.

TABLE OF CONTENTS

ILLUSTRATIONS

TABLES

/1550

Introduction

The Transportation Technology Center at Sandia National Laboratories (SNL/TTC) initiated a program in conjunction with Battelle Pacific Northwest Laboratories (PNL) to benchmark thermal and structural codes that are available to the nuclear material transportation community. This program consists of five phases. During the first phase, publicly available codes were inventoried and reviewed. Following the review, a limited number were selected for further evaluation. The second phase involved the development of a series of cask-like impact problems. The third phase involved the independent solution of the problems by each laboratory. The fourth phase consists of the transfer of information between the laboratories and the nuclear material transportation community. In November 1982 the first Industry/Government Joint Thermal and Structural Codes Information Exchange was held. During this exchange, the results of the code inventory and evaluation were presented and the benchmark problems were defined.[1] This exchange was followed by a second exchange held in October 1984. During this second meeting the numerical analyses of the benchmark problems were presented and an experimental program defined. The fifth phase of the program will involve obtaining reliable experimental data for comparison with the numerical analyses.

This report summarizes the results of the structural benchmarking activity, while a companion report[2] covers the thermal benchmarking. The results that are presented include solutions obtained by Sandia,[3] PNL,[4] GA Technologies[5] and the Century Research Center Corporation[6].

Background

The numerical analysis of structural problems is rapidly expanding and hence there has been a substantial effort

directed at qualitatively evaluating and comparing available codes. Representative papers include Fong (1982)[7] and Dunder and Belonogoff (1980).[8] Fong compares eight finite element codes based on documentation quality, desirable features, user support and availability, element libraries, material libraries, and procedure libraries. Dunder and Belonogoff discuss the factors that should be used in selecting codes. These include service factors, evaluation criteria, program capabilities, efficiency, user convenience and protection, and developer reliability and responsiveness. These papers are of greatest value in establishing evaluation criteria and selecting codes for further evaluation.

There are also studies, of a more quantitative nature, where multiple codes are used to analyze a given problem. These include Crose and Fong (1984)[9] and Ball, et al., (1974).[10] In each of these papers finite element codes were used to analyze a specific problem and the results were compared. Since these papers present no experimental data, they rely on "consensus" solutions for statements of accuracy or applicability.

In addition, there are also papers that address the analysis of the impact of nuclear shipping casks.[11,12,13] Yagawa, et al., (1984)[11] present a set of two end impact problems with plastic deformation and sliding interfaces. Solutions for several codes are presented without experimental confirmation. Adams, et al., (1984)[12] survey the available analytical techniques as well as existing cask designs. Static, dynamic, one-dimensional, and two-dimensional analyses of a steel clad lead cylinder end impact are presented. While this paper provides an excellent survey of existing techniques, it does not provide code specific information or experimental information. Counts and Payne (1977)[13] provided a review of three codes and six end impact tests. The codes were used to

determine the lead slump. While limited in scope, this paper provides a methodology for code benchmarking.

Benchmark Problem Selection

In order to meet the objectives of this program, a benchmark problem set was selected which would be cask-like in nature, test the capabilities of the surveyed codes, and yet be of sufficiently simple geometry that construction of models for experimentation would be straightforward.

The problems chosen for the benchmarking program reflect the regulations concerning the hypothetical accident condition of free drop in 10 CFR 71. This regulation states: "Free Drop--A free drop through a distance of 30 feet onto a flat, essentially unyielding horizontal surface, striking the surface in a position for which maximum damage is expected." This regulation specifies impact velocity and a target rigidity, but leaves the orientation of the package to be determined. Possible impact orientations are shown in Figure 1. Since the cg over corner and arbitrary orientation impacts are inherently three-dimensional, only the end and side impacts will be used in this benchmarking program. This allows evaluation of the various codes' material models and large strains capabilities while maintaining relatively simple geometries.

To adequately model nuclear shipping casks, the codes should include elastic and elastic/plastic material models, sliding interfaces, and large deformation capability. These geometric and materials constraints resulted in the problem set shown in Figure 2.

The parameter values requested from the numerical analyses of these problems were selected so that they could be readily obtained experimentally. The values requested represent those

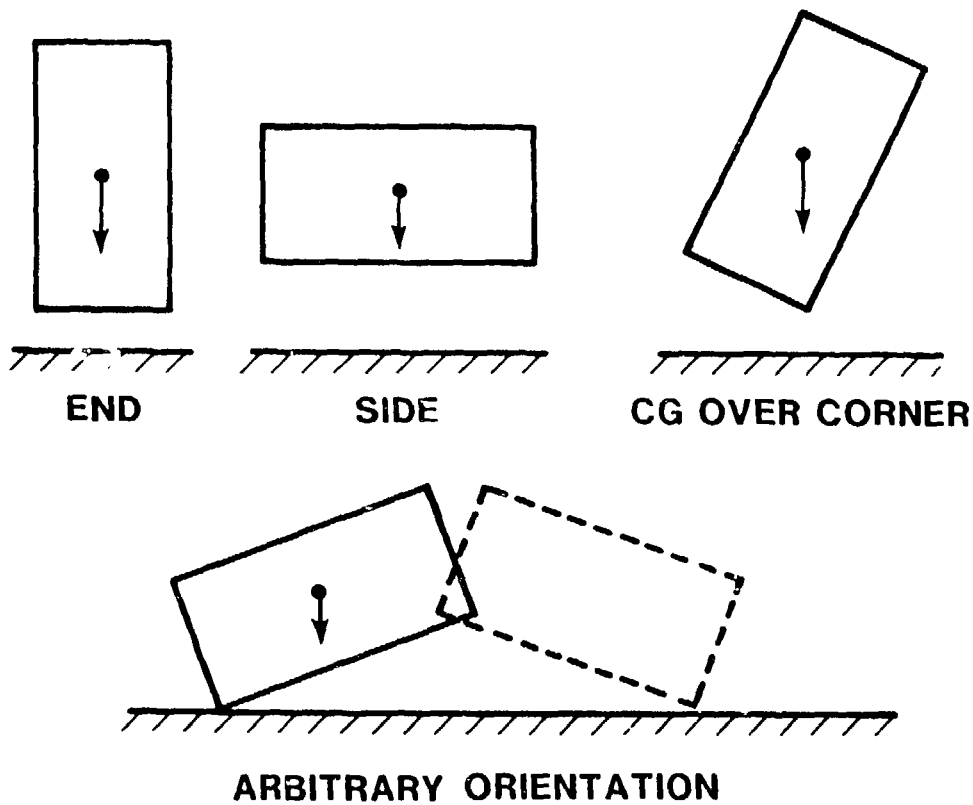

Figure 1: Possible impact orientations

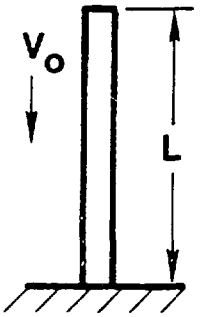

MODEL A - ELASTIC END IMPACT

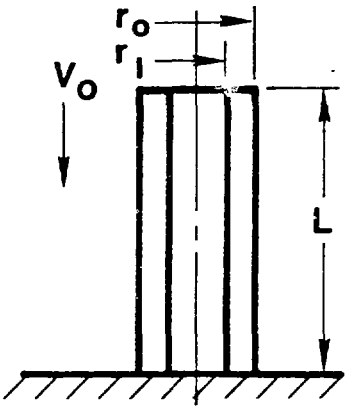

MODEL B - ELASTIC/PERFECTLY PLASTIC END IMPACT

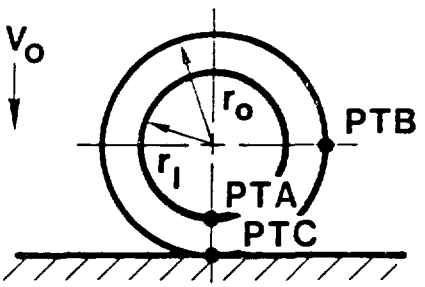

MODEL C - ELASTIC SIDE IMPACT

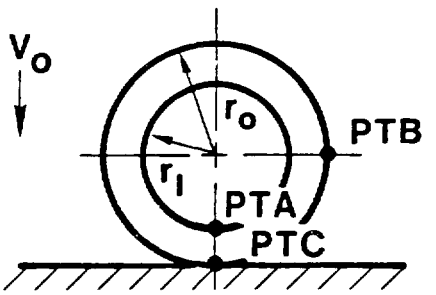

MODEL D - ELASTIC /PERFECTLY PLASTIC SIDE IMPACT

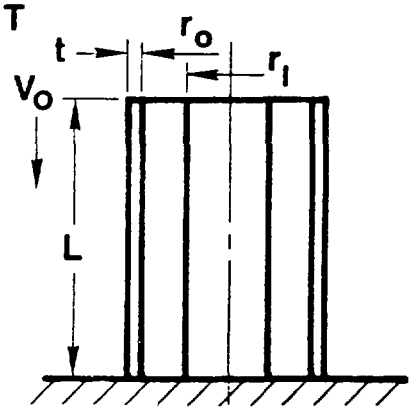

MODEL E - ELASTIC/PERFECTLY PLASTIC END IMPACT WITH SLIDING INTERFACES

Figure 2: Benchmark problem set

that can be obtained using high-speed photometrics measurement, such as impact duration and rebound velocity; those permanent deformations that can be obtained by post-test measurement; and time-dependent values of strain, which can be recorded using strain gages. The time-dependent data are sensitive to the measurement point, as will be shown in the numerical analyses.

While these problems are intended to examine realistic physical phenomena, they are not all inclusive. As has been previously mentioned, three-dimensional problems are not addressed. The problems do not incorporate the separate phenomena associated with impact limiters such as crushable foam behavior, anisotropic material behavior as exhibited by wood, or the buckling of fins. The selected problems also do not attempt to simulate phenomena associated with ferritic casks such as brittle fracture. Even with these exceptions, the problems represent a reasonable first pass at testing the ability of the codes to simulate realistic shipping casks.

Results

The solutions submitted utilized the codes summarized in Table 1. The variety of codes allows comparisons of time integration technique and type of code. In addition, three independent users utilized the HONDO II code. This allows the variation in the HONDO II solutions to be used as a measure of the variability expected from the users as opposed to variability between codes. The tabulated values are reported for each solution as well as the mean and standard deviations for all solutions and for the HONDO II solutions.

TABLE 1

Code Matrix

Code	Type	Time Integration
HONDO II	Finite Element	Explicit
PISCES-2DELK	Finite Difference	Explicit
MANJUSRI-2D	Finite Difference	Explicit
MARC	Finite Element	Implicit
ANSYS	Finite Element	Implicit

Model problem A is shown in Figure 3. This model consists of an elastic steel bar undergoing end impact. This problem is the simplest of the problem set and also has an approximate analytical solution[14] based on Love's theory.[15] The approximation includes a term for radial displacement that is dependent on Poisson's ratio, radial location, and axial displacement gradients. The theory assumes that plane cross sections remain plane and that axial displacement is a function only of time and axial location. Based on this approximate theory, a plot of axial compressive stress as a function of distance from the impacting end at time T/4 is shown in Figure 4. The format for this and all other plots are taken from Reference 1.

The corresponding code solutions for this problem, also at time T/4, are shown in Figure 5 which plots axial compressive stress as a function of distance from the impacting end. These solutions compare well with the analytical solution, though the codes tend to average the stresses near the impacting end where the analytical solution shows stresses oscillating rapidly about the mean.

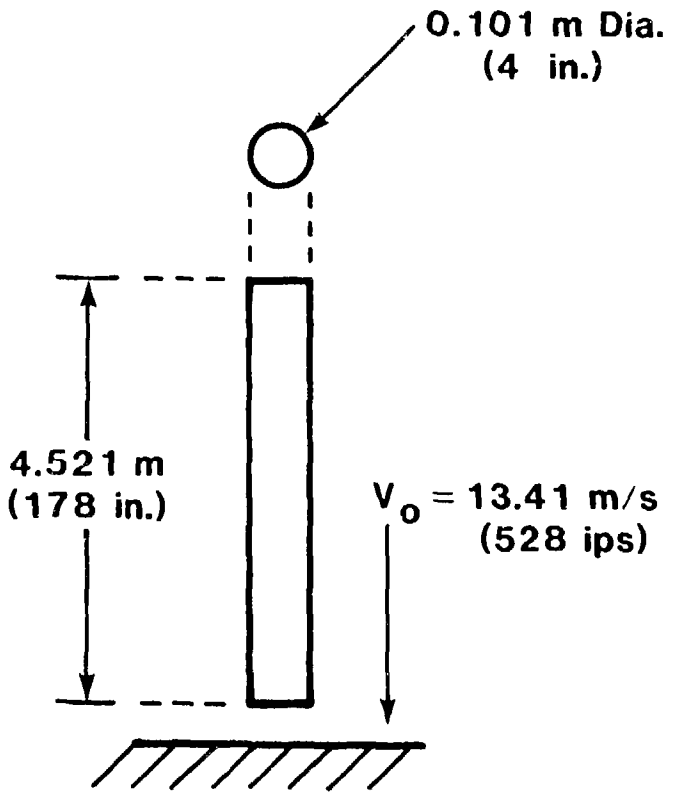

MODEL A - END IMPACT OF ELASTIC ROD

Figure 3: Model problem A--Simulation of an end impact of a linearly elastic rod

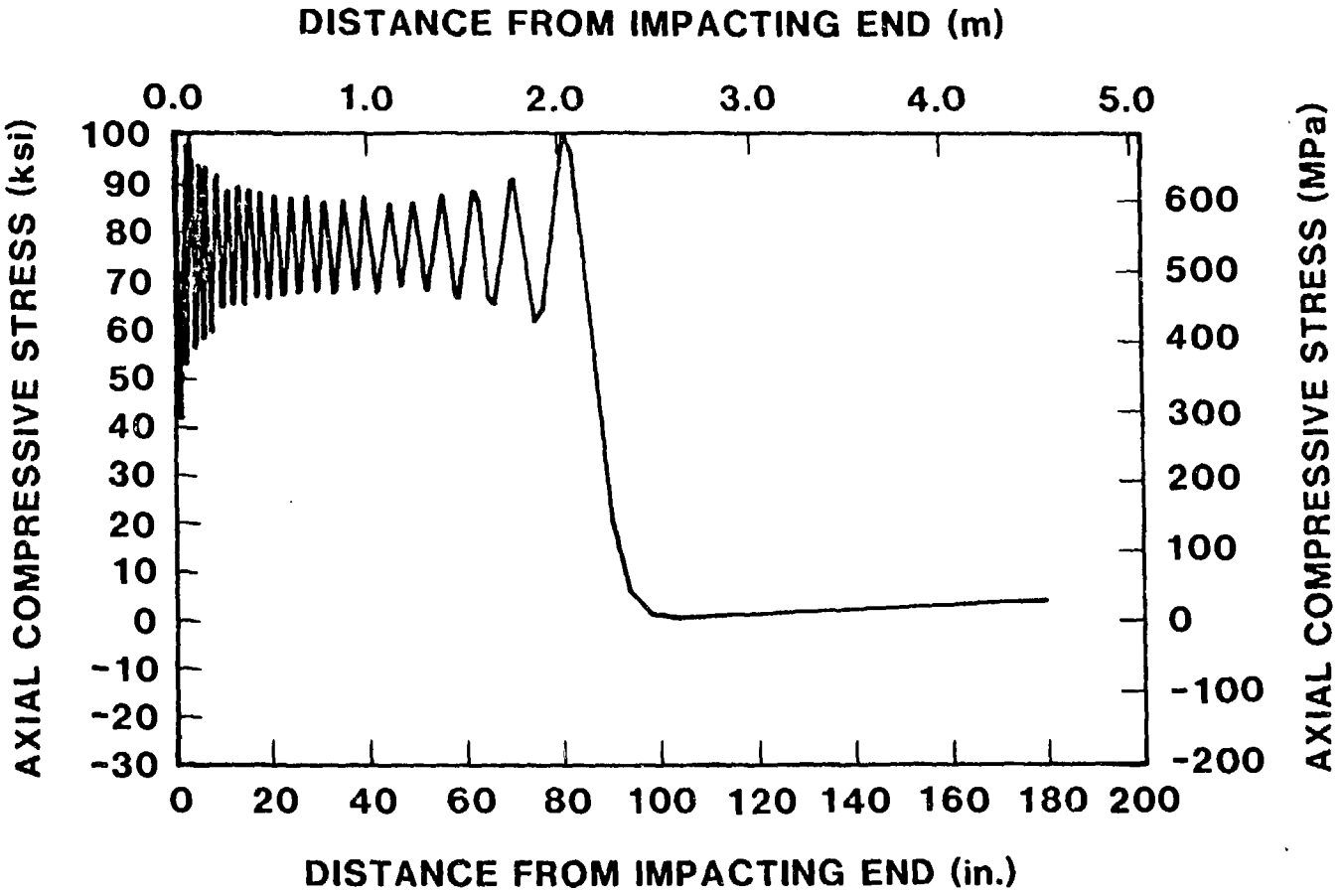

Figure 4: Axial compressive stress based on Love's theory as a function of distance from the impacting end at a time equal to one-fourth of the impact duration for model problem A

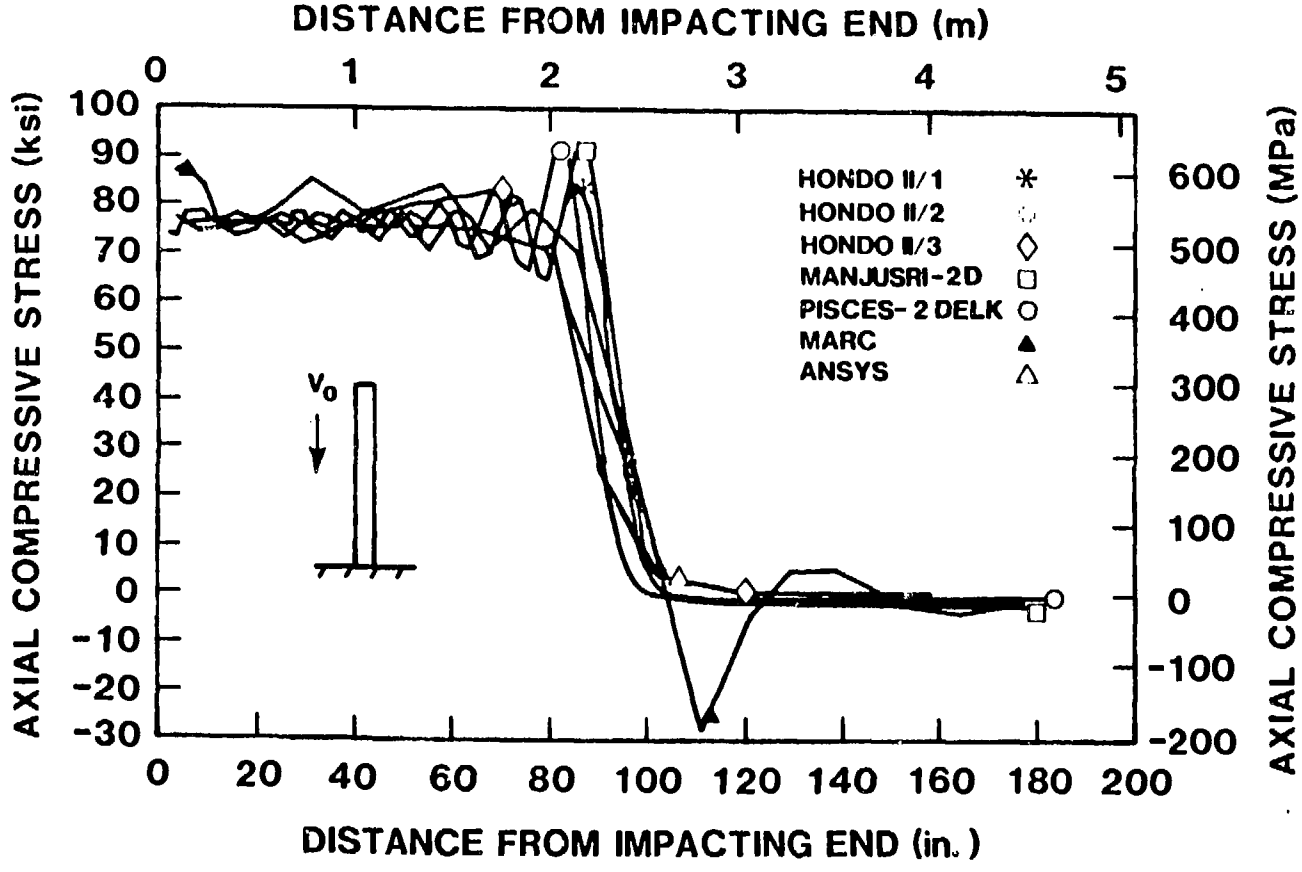

Figure 5: Computed axial compressive stress as a function of distance from the impacting end at a time equal to one-fourth of the impact duration for model problem A

The impact duration, T, and rebound velocities are given in Table 2 with the mean, μ, and standard deviation, σ, values. The small standard deviations indicate that all the codes/users produce reasonably consistent results.

TABLE 2

Model A--End Impact of an Elastic Rod

Code/User	Impact Duration (ms)	Rebound Velocity (m/s)
Hondo II/1	1.86	13.46
Hondo II/2	1.86	13.77
Hondo II/3	1.86	13.1
MANJUSRI-2D	1.89	13.4
PISCES-2DELK	1.88	13.46
MARC	1.84	10.77
ANSYS	1.82	NR*
μ Total	1.86	12.99
σ Total	0.0235	1.11
μ HONDO	1.86	13.44
σ HONDO	0	0.34

*Not reported

Model problem B is shown in Figure 6. This model consists of an annular elastic/perfectly plastic steel cylinder undergoing end impact. This problem tests the ability to solve nonlinear problems involving the behavior associated with plastic deformation. The hoop strain at the outer radius of the impacting end is plotted as a function of time in Figure 7. This plot shows that the introduction of plasticity results in a substantial variation in the strains reported from the various codes. The difference in the strains calculated using HONDO II at 3 ms is 0.006. The corresponding difference using all the codes is 0.018. Further, for the finite element codes the implicit integration codes MARC and ANSYS predict an average strain at 3 ms of less than one-half the explicit

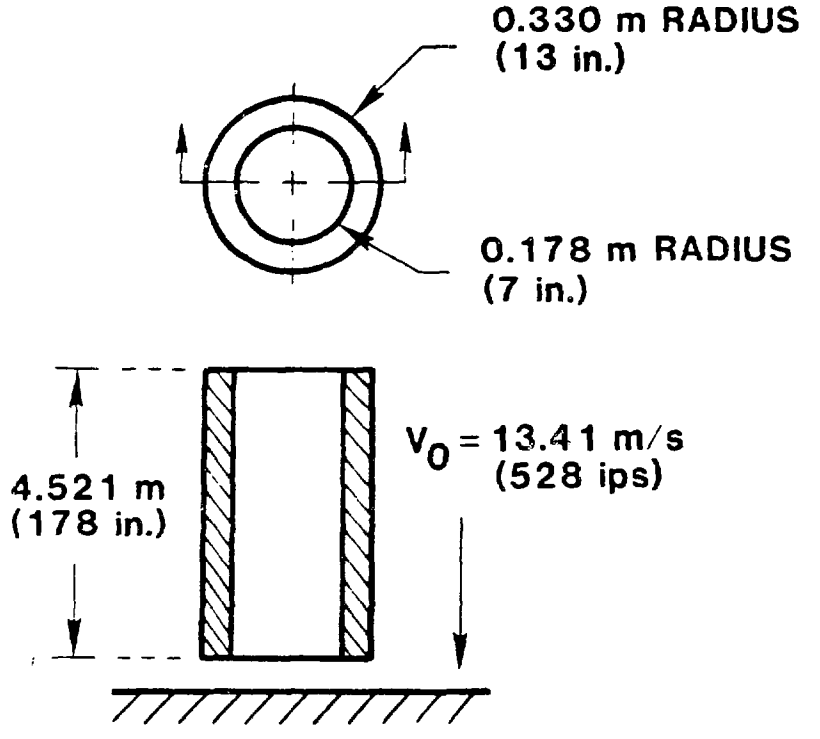

MODEL B - END IMPACT OF AN ELASTIC/PERFECTLY PLASTIC ANNULAR STEEL CYLINDER

Figure 6: Model problem B-Simulating the end impact of an elastic/ perfectly plastic annular steel cylinder

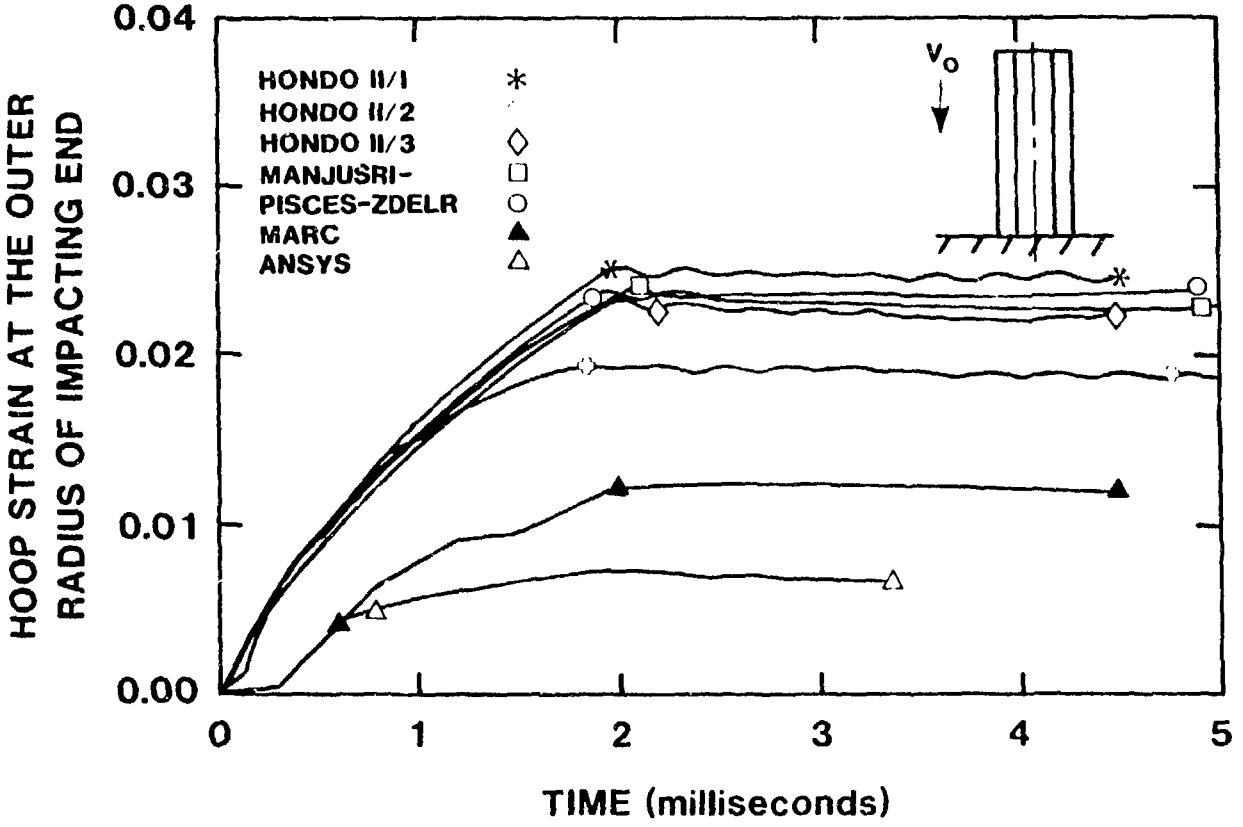

Figure 7: Calculated hoop strain at the outer radius of the impacting end as a function of time for model problem B

integration codes, indicating that the implicit integration schemes generate stiffer systems. Since the HONDO II/3 and ANSYS solutions utilized the same mesh, the difference must be attributed to other causes, such as the greater time step size generally utilized by implicit integration techniques. There is no significant difference in the explicit integration techniques between the finite element and the finite difference solutions.

The tabulated values for impact duration, rebound velocity, and final axial deformation are shown in Table 3. The variation between code type and integration technique for the tabulated values was not significant. This indicates that the impact duration, rebound velocity, and final axial deformation are less sensitive to code and user differences than the strains.

TABLE 3

Model B--End Impact of an Elastic/Perfectly Plastic Annular Steel Cylinder

Code/User	Impact Duration (ms)	Rebound Velocity (m/s)	Final Axial Deformation (m)
HONDO II/1	3.99	3.7	0.0157
HONDO II/2	3.30	4.14	0.015
HONDO II/3	3.907	3.63	0.0137
MANJUSRI-2D	3.47	3.23	0.0173
PISCES-2DELK	3.42	3.07	0.014
MARC	3.96	4.32	0.0138
ANSYS	3.33	NR*	0.0146
μ Total	3.51	3.68	0.0149
σ Total	0.22	0.49	0.00129
μ HONDO	3.45	3.82	0.0148
σ HONDO	0.13	0.28	0.00101

*Not reported

Model problem C is shown in Figure 8. This model consists of an annular elastic steel cylinder undergoing side impact. Plane strain is assumed in this problem. The horizontal stress at the inside radius, point A, is plotted as a function of time in Figure 9. While the figure indicates that the MARC solution

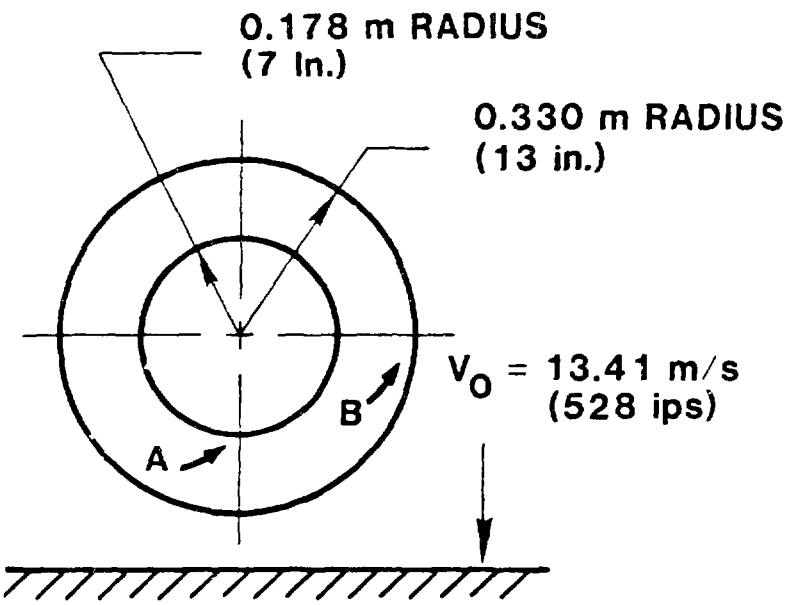

MODEL C - SIDE IMPACT OF AN ELASTIC ANNULAR STEEL CYLINDER

Figure 8: Model problem C-Simulating the side impact of an elastic annular steel cylinder

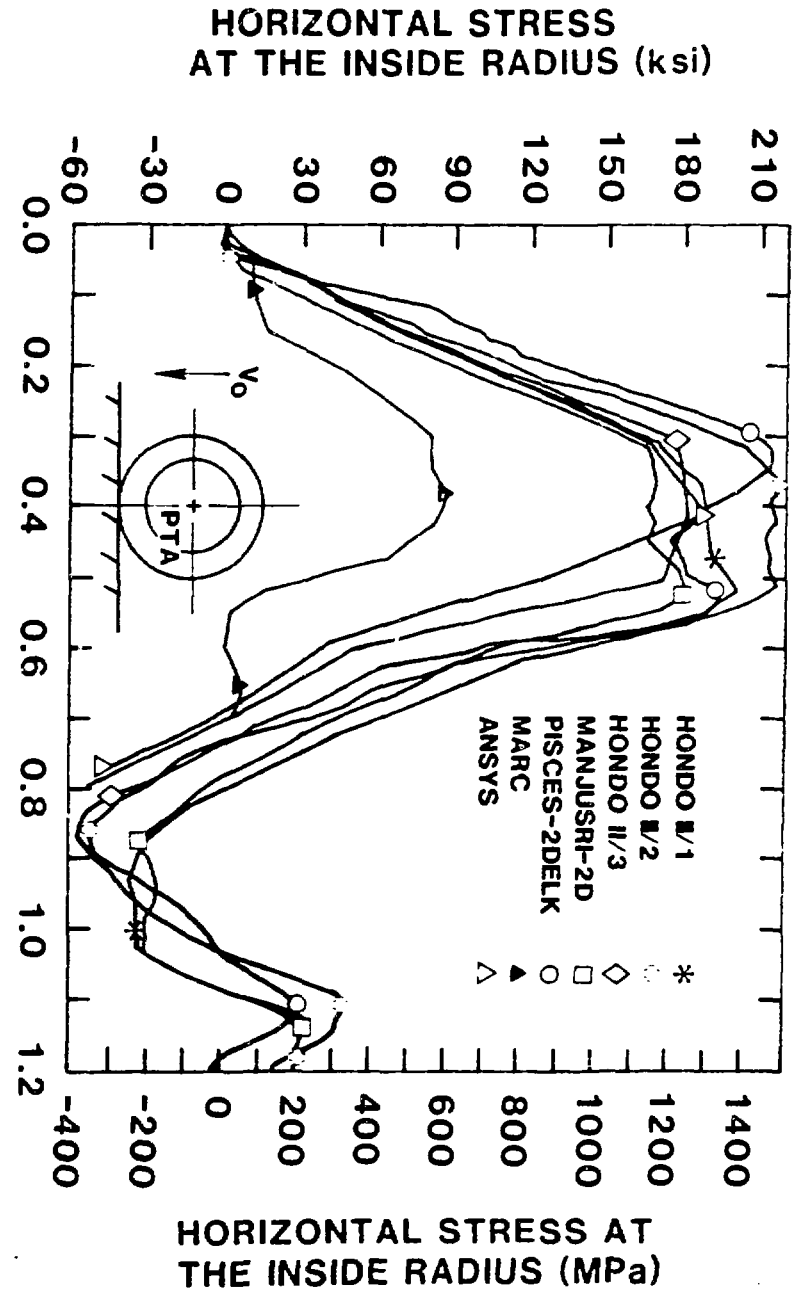

Figure 9: Calculated horizontal stress at the inside radius as a function of time for model problem C

predicts significantly lower stress than the other codes, this is probably an erroneous conclusion. Differences result from the effect of significant variations in the meshes used in the analysis of the problem. The mesh used in the MARC code had three elements through the thickness while the remaining codes used six or seven elements through the thickness at the impacting point. Figure 10 shows meshes used in the HONDO II/2 and MARC analyses. The stresses reported for both of these codes were averaged element stresses. The radial stress gradient for the two innermost HONDO II elements at 0.4 ms is 35,800 MPa/m (132 ksi/in). Using this gradient to correct the MARC solution from the average value at 0.203 m (8 in) to a comparison value at 0.216 m (8.5 in) increases the horizontal stress from 586 MPa (85 ksi) to 1030 MPa (150 ksi). If this same linear correction factor were used to correct to the inner radius it would yield a value of 1500 MPa (217 ksi). These values span the reported values and demonstrate the sensitivity of the solution to the mesh used.

Shown in Figure 11 is the vertical stress at the outside radius, point B, as a function of time. In this problem the variation in maximum vertical stress is 345 MPa (50 ksi). Since this variation is between two of the HONDO II solutions the differences are considered to be user dependent.

The tabulated values of impact duration and average rebound velocity are given in Table 4. The tabular data show no significant code-to-code variability other than that previously discussed.

This problem had high stress gradients due to the geometry of the problem and hence a greater variability due to mesh size and user interpretation was to be expected. This is supported by the variability within the HONDO II solutions.

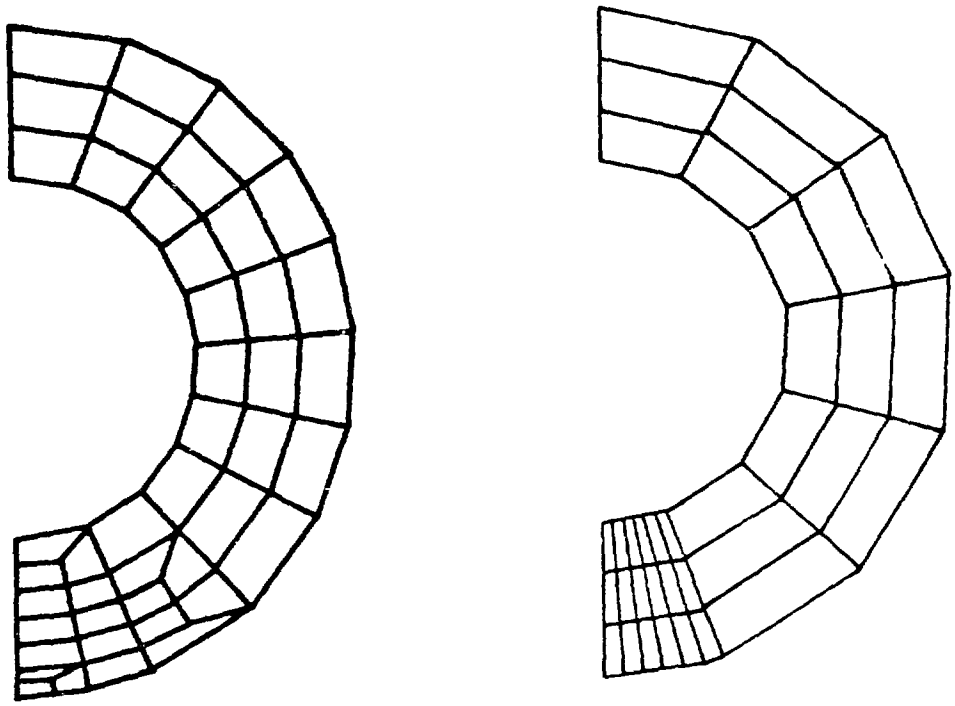

Figure 10: The meshes used in the analysis of model problem C for the Hondo II/2 and MARC analyses

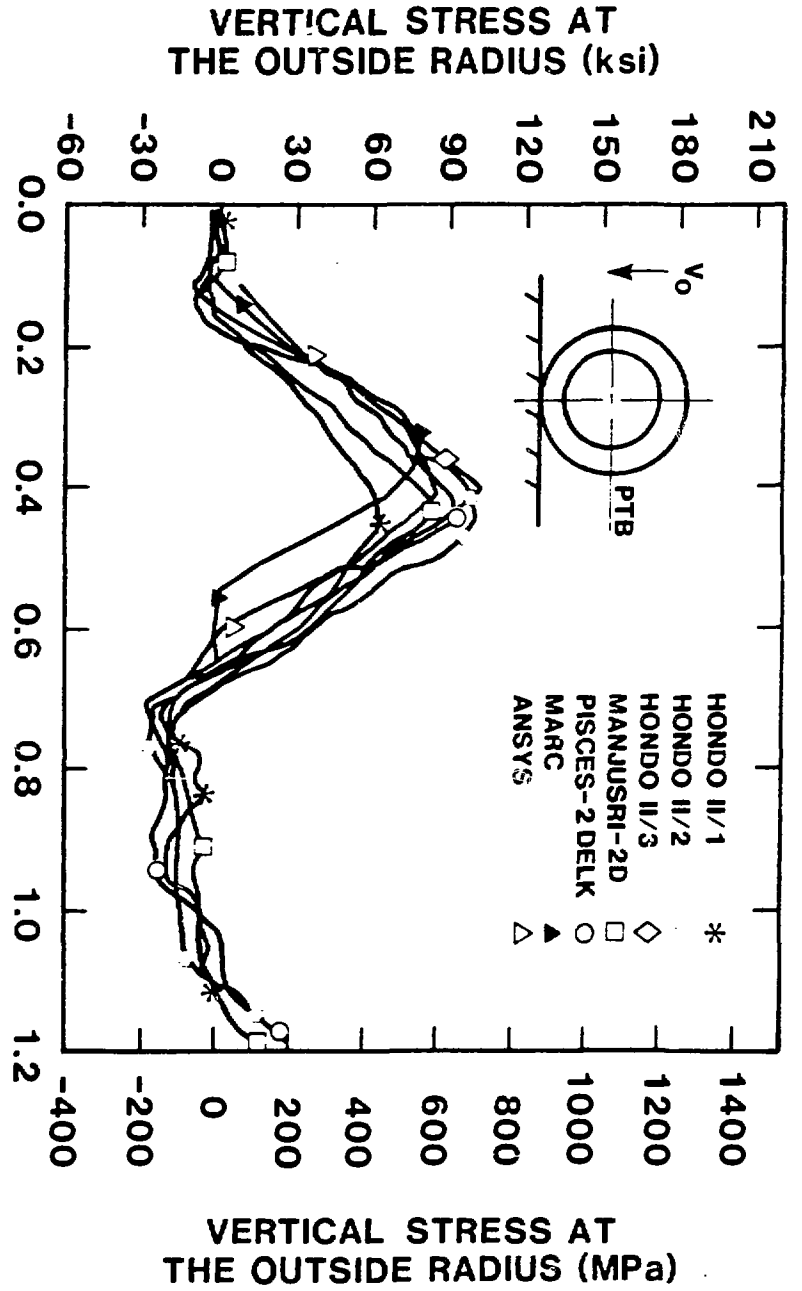

Figure 11: Calculated vertical stress at the outside radius as a function of time for model problem C

TABLE 4

Model C--Side Impact of an Annular Elastic Steel Cylinder

Code/User	Impact Duration (ms)	Rebound Velocity (m/s)
HONDO II/1	0.83	12.96
HONDO II/2	0.77	13.2
HONDO II/3	0.77	12.80
MANJUSRI-2D	0.83	12.0
PISCES-2DELK	0.79	13.4
MARC	0.69	9.14
ANSYS	0.727	NR*
μ Total	0.772	12.25
σ Total	0.0513	1.60
μ HONDO	0.79	12.99
σ HONDO	0.0346	0.20

*Not reported

Model problem D, shown in Figure 12, provides some measure of the effect of plasticity. The geometry, initial conditions, and meshes duplicate model problem C with only the material model changed. The horizontal strain at the inside radius, point A, is plotted as a function of time in Figure 13. The vertical strain at the outside radius, point B, is plotted as a function of time in Figure 14. The meshes used for the finite difference codes were only significantly different in the vicinity of point B. The strains at 0.4 ms varied by a factor of 2. Direct comparison with the finite difference solutions are difficult due to the mesh differences.

The tabular data of impact duration, rebound velocity, and the horizontal and vertical ovalizations are given in Table 5. The horizontal ovalization is defined as the ratio of the change in horizontal outside diameter to original diameter with a similar definition for the vertical ovalization. These data

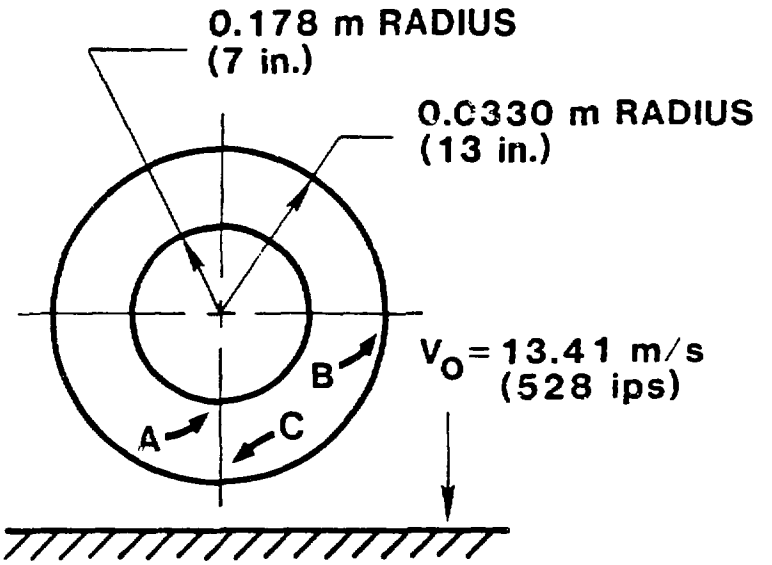

MODEL D - SIDE IMPACT OF AN ELASTIC /PERFECTLY PLASTIC STEEL CYLINDER

Figure 12: Model problem D-Simulating the side impact of an elastic/perfectly plastic steel cylinder

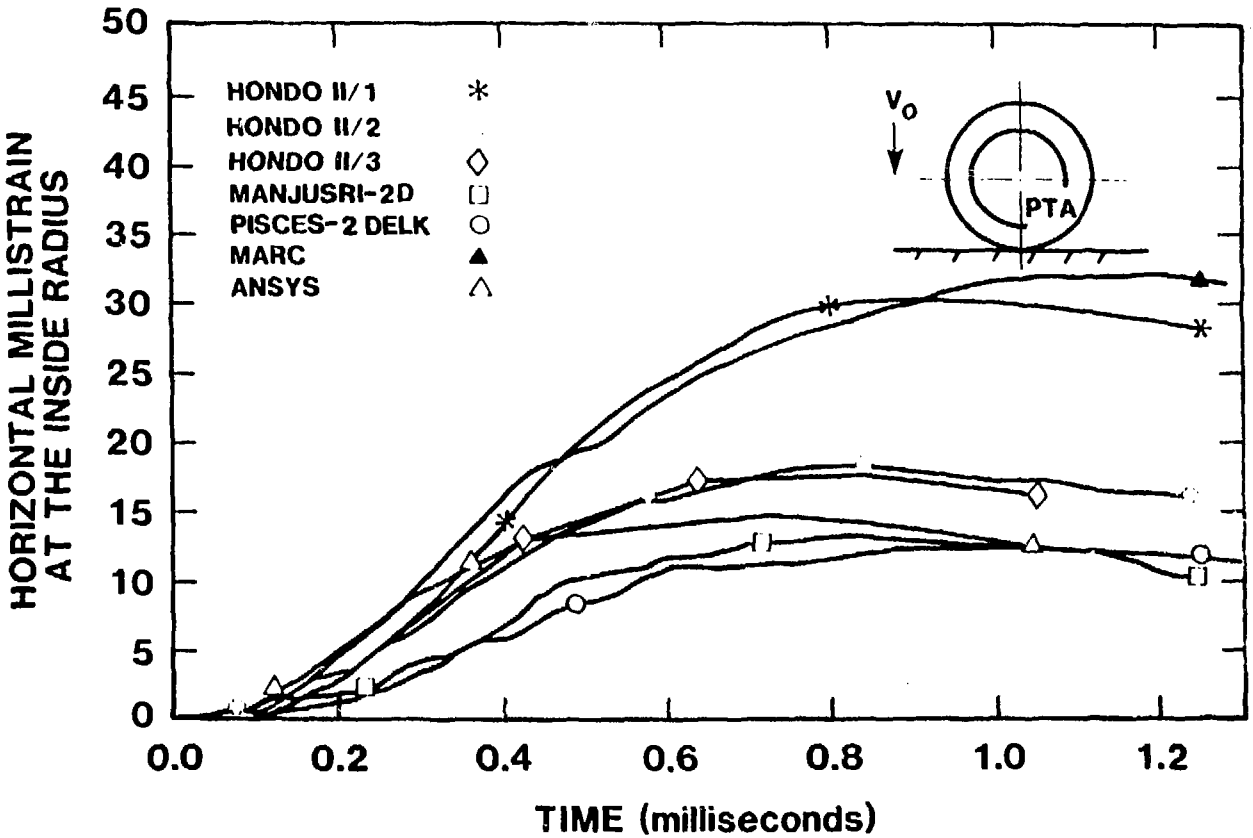

Figure 13: Calculated horizontal strain at the inside radius as a function of time for model problem D

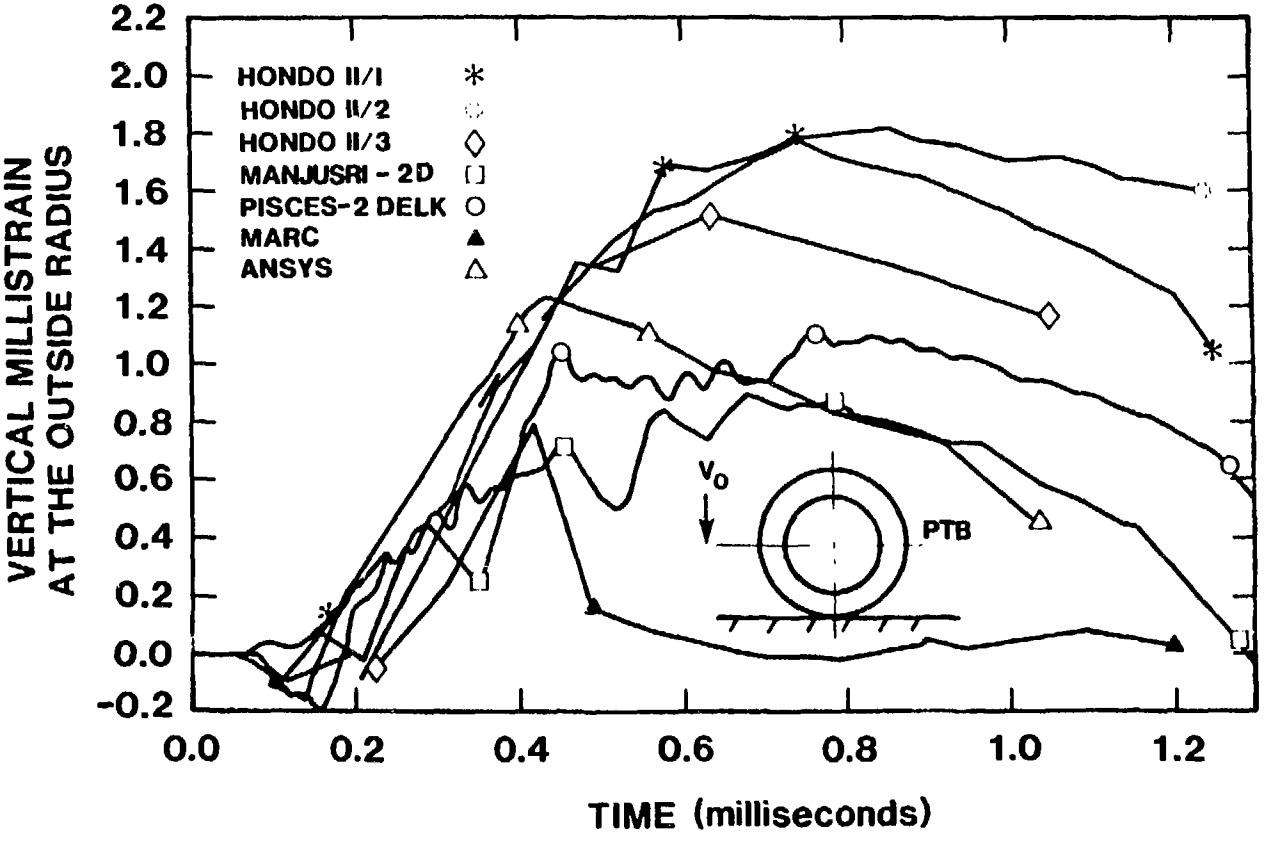

Figure 14: Calculated vertical strain at the outside radius as a function of time for model problem D

demonstrate two characteristics of this problem. These are: 1) permanent deformations are low, indicating that the problem is substantially elastic, and 2) the standard deviations of the horizontal and vertical ovalizations are 18 and 24 percent of the mean indicating substantial variability in the plastic portion of the problem. The variability of the impact duration and rebound velocities are similar to those of the purely elastic problem.

TABLE 5

Model D--Side Impact of an Annular Elastic/Perfectly Plastic Steel Cylinder

Code/User	Impact Duration (ms)	Rebound Velocity (m/s)	Horizontal Ovalization (%)	Vertical Ovalization (%)
HONDO II/1	1.15	NR*	0.31	-0.93
HONDO II/2	1.06	3.81	0.27	-0.8
HONDO II/3	1.052	3.378	0.36	-0.746
MANJUSRI-2D	1.20	3.84	0.27	-0.93
PISCES-2DELK	1.19	3.6	0.321	-0.95
MARC	1.10	NR*	0.15	-1.17
ANSYS	0.9886	NR*	0.27	-0.695
μ Total	1.11	3.66	0.28	-0.89
σ Total	0.068	0.21	0.066	0.16
μ HONDO	1.09	3.68	0.31	-0.83
σ HONDO	0.055	0.26	0.045	0.090

*Not reported

Model problem E is shown in Figure 15. This model consists of an elastic/perfectly plastic steel clad annular lead cylinder. The lead and steel are attached at a single point at the impacting end of the cylinder with frictionless surfaces elsewhere. The model problem simulates a sliding interface.

Shown in Figure 16 is the axial compressive strain in the lead at the impacting end as a function of time. The hoop

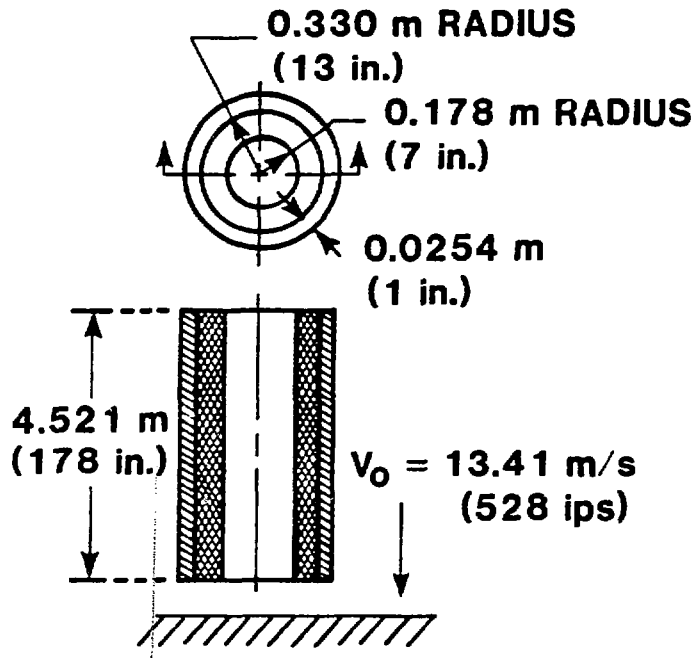

Figure 15: Model problem E-Simulating the end impact of a steel clad annular lead cylinder with elastic/perfectly plastic material behavior

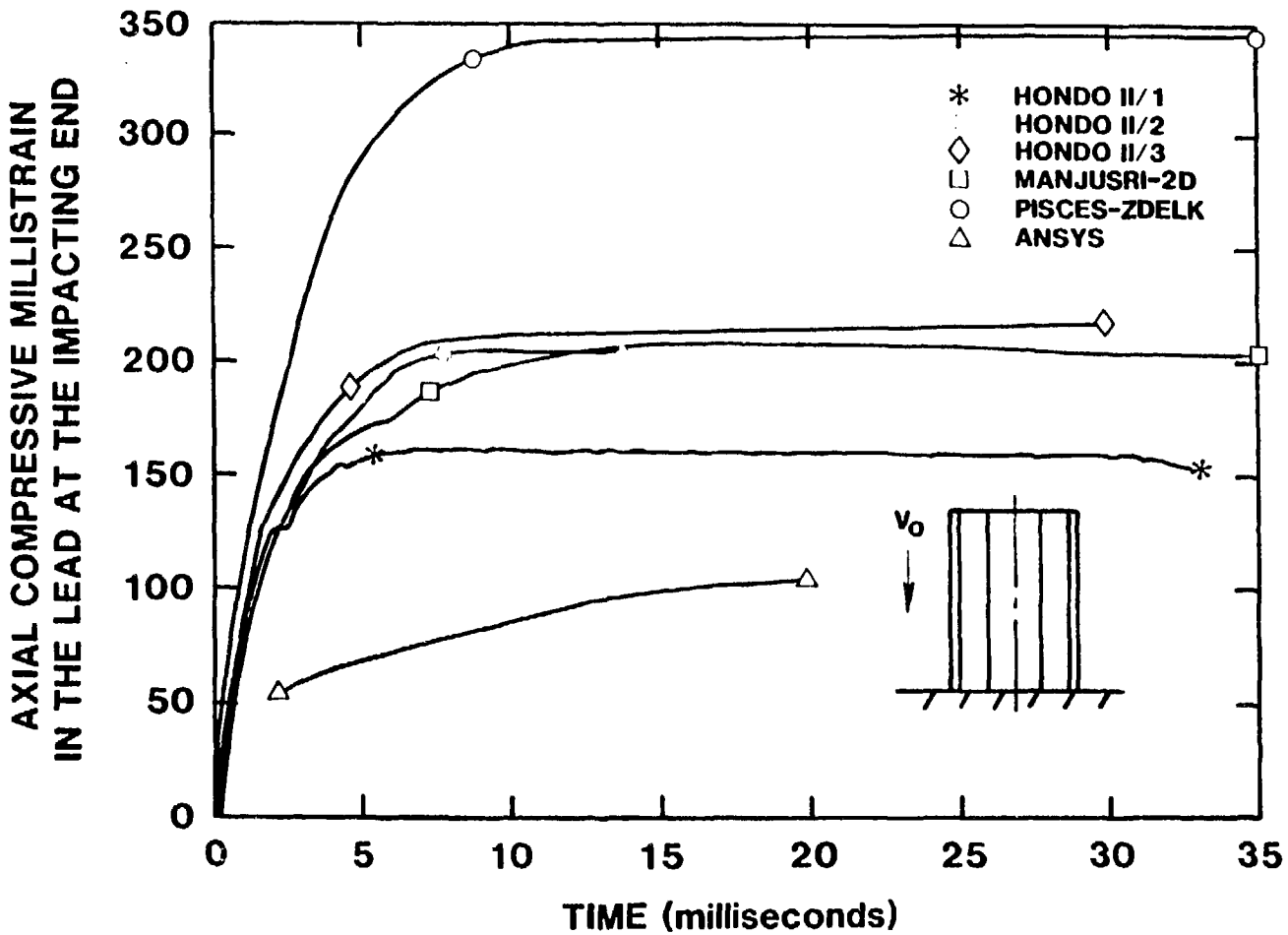

Figure 16: Calculated axial compressive strain in the lead at the impacting end as a function of time for model problem E

strain in the cladding at the impacting end is shown as a function of time in Figure 17. These plots show differences in predicted strain in excess of 100 percent. Without further test problems, it is unclear what portion of the difference is due to plasticity and what portion is due to the sliding interfaces. It should be noted that the implicit integration scheme provided the lowest strains and hence the stiffest system of the finite element codes. The meshes used for the finite element codes were all similar and the meshes used in the finite difference codes were identical, so that these did not account for the observed differences.

The tabular data including impact duration, rebound velocity, and axial deformations are given in Table 6.

TABLE 6

Model E--End Impact of an Elastic/Perfectly Plastic Steel Clad Annular Lead Cylinder

Code/User	Impact Duration (ms)	Rebound Velocity (m/s)	Axial Lead Deformation (m)	Axial Steel Deformation (m)
HONDO II/1	30.0	NR*	0.192	0.0184
HONDO II/2	32.5	1.27	0.19	0.0178
HONDO II/3	30.2	0.804	0.198	0.018
MANJUSRI-2D	27 2	0.75	0.16	0.016
PISCES-2DELK	30.2	0.86	0.20	0.021
MARC	NR*	NR*	NR*	NR*
ANSYS	23.6	NR*	0.117	0.0328
μ Total	28.6	0.97	0.18	0.021
σ Total	3.11	0.24	0.033	0.006
μ HONDO	30.9	1.08	0.193	0.0181
σ HONDO	1.39	0.34	0.004	0.0003

*Not reported

The tabular data and particularly the axial steel deformation reflect a higher degree of variability than that seen in the previous plastic analyses. This indicates that the axial steel deformation in this problem is sensitive to code differences.

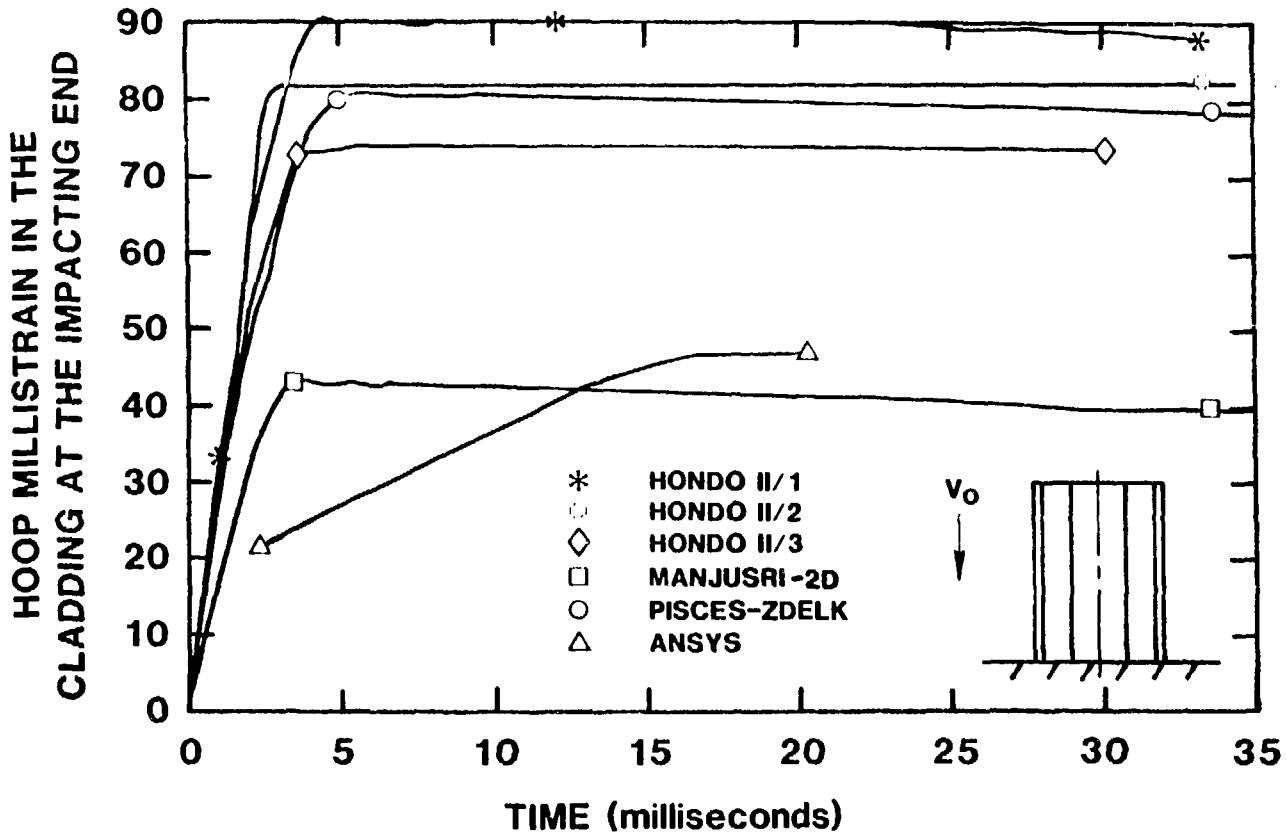

Figure 17: Calculated hoop strain in the steel cladding at the impacting end as a function of time for model problem E

In these data the ANSYS implicit integration scheme seems to produce a stiffer system as seen in the low impact duration and lead slump. The high steel slump results directly from the stiffer lead behavior and is not due to a less stiff steel.

Conclusions

The following observations are made based on the results from the model problems:

1. All of the codes provide good agreement with the analytical solution of elastic model problem A.

2. The variability in elastic model problem C probably results from user-controlled parameters such as mesh size as opposed to code-to-code differences.

3. For the elastic/perfectly plastic model problems B and E, the implicit integration schemes produce stiffer systems than the explicit integration schemes.

4. The impact duration and rebound velocity are less sensitive than the strains to code/user differences in the elastic/perfectly plastic analyses.

5. The introduction of a sliding interface in model problem E yields higher code-to-code variability in the axial steel deformation than was seen in model problem B.

These observations indicate that all of the codes provide consistent answers to the elastic problems within the variability introduced by user-controlled parameters. This indicates that a high degree of confidence can be placed in carefully run and interpreted elastic analyses. The observations also indicate that the introduction of plasticity

results in substantial variability due both to user-controlled parameters and interpretation and to code-to-code variability. This variability is most apparent in the calculated strains. Finally, the observations indicate that inclusion of a sliding interface produces additional variability in the final axial deformation of the steel.

The lack of a "consensus" solution in problems involving plastic deformation and sliding interfaces demonstrates the need to determine the effects of the user-controlled parameters and to obtain experimental data to complete the benchmarking of the codes. The parameters, which remain to be fully investigated, include mesh size, time step size, and convergence criteria. The experiments required are outlined in the following section.

Future Work

The primary objective in the proposed experiments is to obtain data which can be used in benchmarking codes with elastic/plastic material models and large deformation capability. To attain this objective, the proposed experiments will be scaled versions of model problems B and D. This will allow both end and side impact to be examined.

A secondary objective of this study will be the verification of existing scaling laws.[16] To meet this objective, a range of scaling factors will be used in designing the experiments. This will result in multiple versions of each model with variation only in the geometric scaling factors.

The experimental phase of this program should provide sufficient data to complete the benchmarking of structural codes with elastic/plastic material models and large deformation capability.

References

1. Nelsen, J. M. (ed), Industry/Government Joint Thermal and Structural Codes Information Exchange Meeting, Sandia National Laboratories, Albuquerque, NM, 1984.

2. Sanchez, L. C., Performance Testing of Thermal Analysis Codes for Spent Fuel Casks, SAND84-1854A, Sandia National Laboratories, Albuquerque, NM, 1984.

3. Lewis, B. A. and Gwinn, K. W., Evaluation of Computer Programs Used for Structural Analyses of Impact Response of Spent Fuel Shipping Casks, SAND83-0319, Sandia National Laboratories, Albuquerque, NM, 1984.

4. Friley, J. R., Comparison of Structural Computer Programs Used for the Analysis of Impact Response of Spent Fuel Shipping Casks, TTC 0306 PNL 4161, Battelle Pacific Northwest Laboratories, Richland, WA, 1984.

5. Private correspondence with R. Grenier and P. Rasmusson, August 8, 1983

6. Private correspondence with Hideo Obata and Masaharu Itoh, May 14, 1984

7. Fong, H. H., "An Evaluation of Eight U.S. General Purpose Finite-Element Computer Programs" Paper #82-0699-CP, 23rd AIAA/ASME/ASCE/AHS Structures, Structural Dynamics and Materials Conference, May 10-12, 1982, New Orleans.

8. Dunder, V. F. and Belonogoff, G., "Comparing Finite Element Programs in Engineering," Proc. Conference on Finite Element Methods and Technology, March 1980, Pasadena, CA.

9. Crose, J. G. and Fong, H. H., "Finite Element Analysis of a Finite-Strain Plasticity Problem," Nuclear Engineering and Design, Vol. 78, 1984.

10. Ball, R. E., Hulka, W. F., Huffington, Jr., N. J., Underwood, P., and Von Riesemann, W. A., "A Comparison of Computer Results for the Dynamic Response of the LMSC Truncated Cone," Computers and Structures, Vol. 4, 1974.

11. Yagawa, G., Ohtsubo, H., Takeda, H. Toi, Y., Aizawa, T., and Ikushima, T., "A Round Robin on Numerical Analyses for Impact Problems," Nuclear Engineering and Design, Vol. 78 1984.

12. Adams, C. R., Biffle, J. H., Gubbels, M. H., and Huerta, M., A Comparison of Analytical Techniques for Analyzing a Nuclear-Spent-Fuel Shipping Cask Subjected to an End-On Impact, SAND80-1870, Sandia National Laboratories, Albuquerque, NM, June 1981.

13. Counts, J., and Payne, J. B., Evaluation of Analysis Metals in Type B Shipping Container Impact Problems, LA-6640-MS, Los Alamos National Laboratories, Los Alamos, NM, January 1977.

14. Conway, H. D., and Jakubowski, M., "Axial Impact of Short Cylindrical Bars," Journal of Applied Mechanics, December 1969.

15. Love, A. E. H., A Treatise on the Mathematical Theory of Elasticity, Dover Publications, 1944.

16. Duffey, T.A., "Scaling Laws for Fuel Capsules Subjected to Blast, Impact, and Thermal Loading," Proceedings of the 1971 Intersociety Energy Conversion Engineering Conference, Boston, MA, 1971.

DISTRIBUTION

No. of Copies

U. S. Department of Energy
Attn: Larry G. Blalock
Oak Ridge Operations Office
Post Office Box E
Oak Ridge, TN 37830

U. S. Department of Energy
Attn: R. B. Chitwood
Washington, DC 20545

U. S. Department of Energy
Attn: F. P. Falci
Washington, DC 20545

U. S. Department of Energy
Attn: R. F. Garrison
Mail Stop B107
Washington, DC 20545

U. S. Department of Energy
Attn: K. Golliher
Albuquerque Operations Office
Albuquerque, NM 87115

U. S. Department of Energy
Attn: J. J. Jicha
Washington, DC 20555

U. S. Department of Energy
Attn: J. M. McGough
Albuquerque Operations Office
Albuquerque, NM 87115

U. S. Department of Energy
NE-320
Attn: Austin E. Wiles
Washington, DC 20545

No. of Copies

Charles R. Tilford
National Bureau of Standards
A149 Metrology
Washington, DC 20234

L. E. Steele
Code 6390
Naval Research Laboratories
Washington, DC 20375

G. E. Giles
Oak Ridge National Laboratory
Martin Marietta Energy
System, Inc.
Post Office Box X
Oak Ridge, TN 37831

C. V. Parks
Oak Ridge National Laboratory
Martin Marietta Energy
System, Inc.
Post Office Box X
Oak Ridge, TN 37831

L. B. Shappert
Oak Ridge National Laboratory
Martin Marietta Energy System, Inc.
Post Office Box X
Oak Ridge, TN 37831

W. C. Stoddart
Oak Ridge National Laboratory
Martin Marietta Energy System, Inc.
Post Office Box X
Oak Ridge, TN 37831

G. E. Whitesides
Oak Ridge National Laboratory
Martin Marietta Energy System, Inc.
Post Office Box X
Oak Ridge, TN 37831

27 DOE Technical Information Center

No. of
Copies

Frank Zapp
Nuclear Standards Management
Center
Oak Ridge National Laboratory
Post Office Box Y
Oak Ridge, TN 37830

Donald R. Hopkins
U. S. Nuclear Regulatory
Commission
Mail Stop 1130-SS
Washington, DC 20555

Edward Pobolak, Jr.
U. S. Nuclear Regulatory
Commission
Washington, DC 20555

No. of
Copies

Dr. Jeffrey Fong
Center for Applied Mathematics
U. S. Department of Commerce
National Bureau of Standards
Washington, DC 20234

Charles McDonald
U. S. Nuclear Regulatory
Commission
Division of Fuel Cycle and Materials
Licensing
Mail Stop 396-SS
Washington, DC 20555

Dr. G. H. Weidenhamer
U. S. Nuclear Regulatory Commission
Office of Research
Washington, DC 20555

FOREIGN

Hideo Obata
Group 42
Century Research Center Corp.
Ozu-Honkan Building
2, Nihonbashi-Honcho 3-chome
Chou-ku, Tokyo 103 JAPAN

Sandia National Laboratories

	313	J. T. Schamaun
5	3141	C. M. Ostrander
	3151	W. L. Garner
	6320	J. F. Ney
	6323	G. C. Allen
5	6322	R. E. Glass
	6321	R. E. Luna
	6322	J. M. Nelsen
	6322	W. E. Wowak
	6324	B. D. Zak
	6340	R. M. Jefferson
	8024	M. A. Pound

Pacific Northwest Laboratory
Battelle Boulevard
Post Office Box 999
Richland, WA 99352
M. C. C. Bampton
M. J. Budden
J. R. Friley
D. S. Trent